Title

Pengju Jin, Siddhartha Srinivasa

Abstract—Abstract Goes here

I. INTRODUCTION

Detection and identification using artificial landmarks has long been used in augmented reality and computer vision applications. Over the last decade, there has been numerous marker systems, such as ARTags, Apriltags, and Rune Tags, designed to improve detection encoding precision. However, these systems are not robust enough to be used reliability in many robotic applications.

Compared to markerless detection algorithms, these fiducial marker methods are simpler and more consistent. There has been significant effort in improving the detection speed and encoding accuracy. They have yield great results for computer vision tasks that require high detection accuracy like camera calibrations, 3D reconstruction. Furthermore, they have gained popularity in the robotic community for having unique characteristics of high detection rates and numerous encoding schemes. For example, Apriltags are commonly used to test SLAM systems or finding ground truth for objects in manipulation and motion planning tasks as shown in Figure ??.

Despite all the improvements, obtaining accurate pose estimations from these tags remain a challenge. This is especially important for robotic applications because small errors can cause large system failures as the errors propagate and amplify through the system. Currently, these systems yield good results under well conditioned or rendered environments, but this does not translate to ill-conditioned settings. For instances, when Apriltags are used with low resolution camera or harsh lighting conditions, the system often produce poses with tremendous rotational errors as shown in Figure 2. In fact, we observe that the localization accuracy of this system perform significantly worse at difficult viewing angles or when there are noise in the scene. This is a difficult problem because RGB sensors are sensitive to lighting and current fiducial systems are not designed to take advantage of other sensors commonly available on robots.

We present two main contributions in this paper. First, we conducted an in-depth analysis on the effect of various noises on the pose estimation process. In particular, the noise in RGB images creates a perspective ambiguity problem that makes the pose estimation challenging without additional information. Second, we describe a novel method that takes advantage of the RGBD sensors that are commonly available on most robotic systems to accurately estimate the pose from a single tag under noisy conditions in real time. In the core of the algorithm, we recognize that RGB and depth sensors work optimally under different conditions. Therefore, their strength can be combined meaningfully to improve the
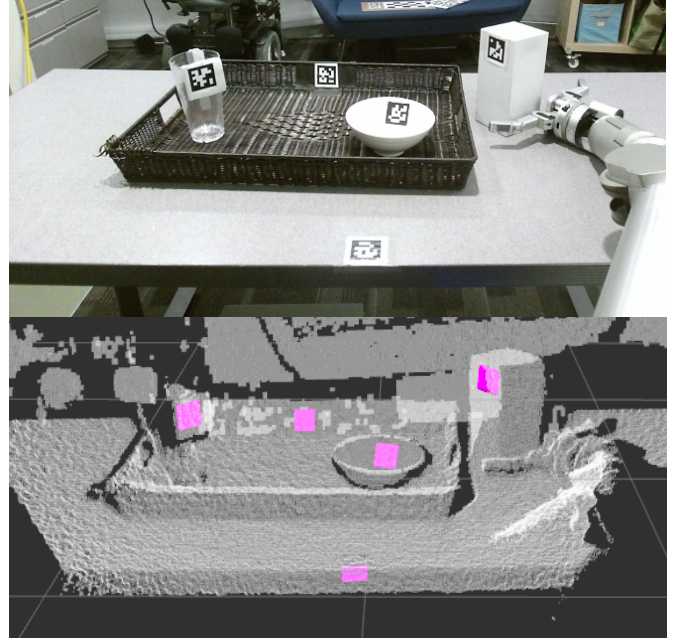

Fig. 1: Apriltag used to localize objects in mainpulation tasks

localization accuracy robust to illumination. There are few key features to this algorithm:

- This method is highly robust to noise in the scene. It can obtain accurate poses suitable for a wide range robotic applications.
- It is easily generalizable to most fiducial tags designs.
- It performs at worse at least as good as using only RGB images.
- It has very small computation overhead and can be ran in real time.

This paper also presents empirical results demonstrating the the successful performance of the algorithm on captured data from an humanoid robot. Our implementation of the algorithm is based off of the Apriltag detection pipeline and it is integrated with ROS.

II. RELATED WORK

Although there are an abundance of fiducial markers, most of them focus on detection and decoding tags using RGB data. The strength of using RGB data is obvious, the color information makes the pattern detection process much simpler. They are typically designed with a specific binary pattern to encode information in the inner region. There are two large type of common tags: square tags and circle tags.

ARTags[], Aruco[], ARToolkit[], AprilTag[] and AprilTag 2[] are examples of squared based fiducial tags. The perspective projection of a square becomes a general quadrilateral

which can be computed easily using any contour tracing algorithm. Given the scale of a single marker, the full 6-DOF pose can then be estimated using the corners of the quadrilateral. AprilTag and AprilTag2 both use a binary payload that guarantees a minimum Hamming distance between tags. Recently AprilTag 2, built upon the origin Apriltag and ARTag system, also implemented a new boundary segmentation algorithm which gained significant computation speed. Therefore, the advantages of the square tags are that they can be located very efficiently and they have reliable decoding schemes. However, since they are detected using rectangles and lines, the accuracy of their corner point sub-pixel locations are limited. This downfall cause them to have poor pose estimation results under occlusion and image distortion.

On the other hand, circular tags are created to encode the payload using small circles. The example or circular tags include Concentric Circle, Intersense and Rune tags. The perspective transformation of a circle is an ellipse, which can be used to directly compute the pose using back projection methods. The detection of circular features are more accurate to localize and thus generates better pose estimations. However, small circular features become hard to detect when they are far away from the camera and thus their effective range is smaller than that of square tags. Furthermore, Rune tags and Pi tags have significantly higher computation cost to decode their pay load.

III. Challenges

In square fiducial marker detection, the pose is calculated by using the four corners of the tag. Since the tags are planar, it is easy to compute perspective point correspondences from the corners. This can be formalized as a specific case of the Perspective-N-Point problem and it has been well studied in geometry based Computer Vision literatures [][]. There are numerous optimization methods such as ones purposed in [] and [] to solve this problem. In particular, in [], the author shows that there is a deterministic solution to the Perspective-4-Point (P4P) problem. In other words, given the projection of a tag's 4 corners, the pose of the tag is unique. In practice, however, when a tag is captured in a low resolution camera, this method is very sensitive to noise. For instances, when ARTags, Apriltags and ARToolkit systems are used in scenarios shown in Figure **??**, the poses of the tags alter when the scene is static. Since the minimal number of perspective points are used to estimate the pose, a small variance in the corner detection process will yield estimations far from the true pose as shown in Figure 2.

We will illustrate the ambiguity effect by using two over lapping cubes in Figure 3. The overlapping face of the two cubes are interlaced but rotated by 120 degrees. However, due to perspective projection, the squares appears to be on the same plane. Under low camera resolution, the over lapping squares become virtually indistinguishable. The red circular regions are the detected corners under some sensory noise. Even though the reprojection error is minimized in the 2D space using P4P optimization methods, the 3D pose
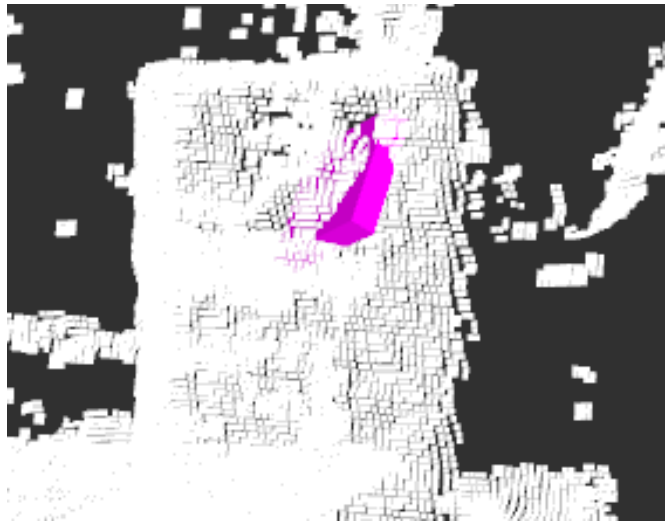

Fig. 2: The orientation of Apriltag placed on the object is greatly misaligned with the actual object
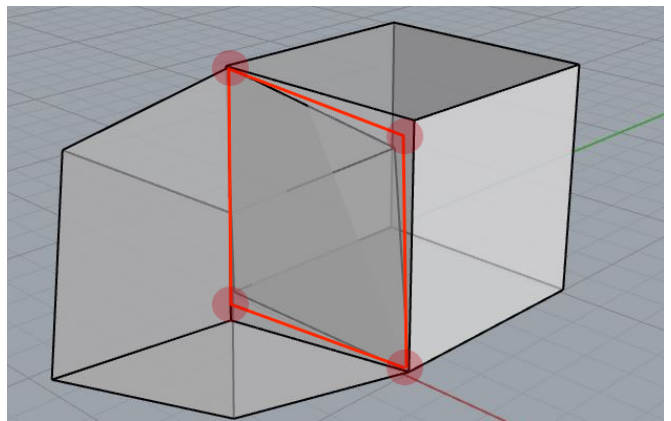

Fig. 3: Perspective Ambiguity illustrated with overlapping cubes

can still be far off. The result of the optimization can be characterized as a bimodal distribution and a function of the the viewing angle. Depending on the noise level in the scene, the optimization might converge to either one of the local minimum causing the pose estimation to be unreliable.

IV. Approach

This section describes a method for accurately estimating poses for square fiducial tags in noisy settings by fusing RGBD data. The process of detecting and decoding the tag is identical to previous methods. This also make our method easily generalizable to any square tag detection systems. However, the detected corners are treated as approximated locations of the true corners. Using the corners, the method implicitly evaluate the depth data and RGB data as two independent observations and fuse them to minimize the error in 2D and 3D space.

There are three distinct components to this method. First, we find the plane in $SO(3)$ containing the tag using depth data and detected corners. Secondly, an approximate initial pose is computed using the depth plane. Finally, the method refines the initial pose using the RGB data by minimizing

the reprojection error within a constrained space. Each component is described in detail in the following subsections.

A. Depth Plane Fitting

With a calibrated RGBD sensor, depth and RGB streams are registered to the same frame. The square patch of points in the depth image defined by the g also contains the range information of the tag. Here we take advantage of the planar characteristic of the tag. By fitting a plane over the range data, we can constrain the pose of the tag to be on the plane.

The raw range data retrieved from the Kinect One sensor are usually noisy as illustrated by Figure 4. Specifically, borders of the tag and some of the dark regions of the tag produce highly unreliable range data. Therefore, we first filter the data by removing points too far from the median before fitting the plane. Nevertheless, the remaining points could have a large variance depending on the lighting condition and the magnitude of the plane rotation. The accuracy of the plane and tag pose is directly affected by the noise level of data. In fact, we want to characterize the uncertainty and weight the initial estimation accordingly during the fusing stage.

In implementation, we used a Bayesian plane fitting algorithm described in [Uncertainty Analysis] which computes the Hessian Normal parameters of a plane through optimizing

$$\min_{\hat{\boldsymbol{n}},d} \sum_{j=1}^{N} \frac{(p_j(\hat{\boldsymbol{n}} \cdot \hat{\boldsymbol{m}_j}) - d)^2}{(\hat{\boldsymbol{n}} \cdot \hat{\boldsymbol{m}_j})^2 \sigma^2\{\bar{p}_j\}} \qquad (1)$$

The algorithm in the paper assumes a radial Gaussian noise in the range data p_j with the standard deviation modeled by a function in the form

$$\sigma\{\bar{p}_j\} = \frac{kd^2}{\|\hat{\boldsymbol{n}} \cdot \hat{\boldsymbol{m}_j}\|} \qquad (2)$$

where $\hat{\boldsymbol{n}}$ is the local normal to the planar surface of the depth point and $\hat{\boldsymbol{m}_j}$ is the measurement direction for the sensor for point p_j. The coefficient $k > 0$ is an estimated value obtained from sensor calibration. In our implementation, we obtained k by simplified the results from [Kinect Noise Model paper].

Another important result we used from [] is the covariance matrix for the plane-parameters. The covariance matrix is obtained by taking the *Moore-Penrose generalized inverse* of Hessian matrix computed from the Lagrangian. The covariance characterizes the uncertainty of the plane and defines the refinement regions of the pose later in the pipeline.

B. Initial Pose Estimation

The pose of the tag can be described as the transformation from tag frame's coordinate system to the sensory frame's coordinate system of the robot given by $[R, \boldsymbol{t}]$. However, the depth plane $D[\hat{\boldsymbol{n}}, d]$ alone is insufficient to determine the transformation because it only defines 3 DOF in a 6 DOF space. Furthermore, the center of the tag must align with the center of the plane and thus further constrain 2 DOF. However, there are still infinite number of valid poses rotating about the normal $\hat{\boldsymbol{n}}$. One solution is to constrain the pose by using a corner as an extra point correspondence to solve for
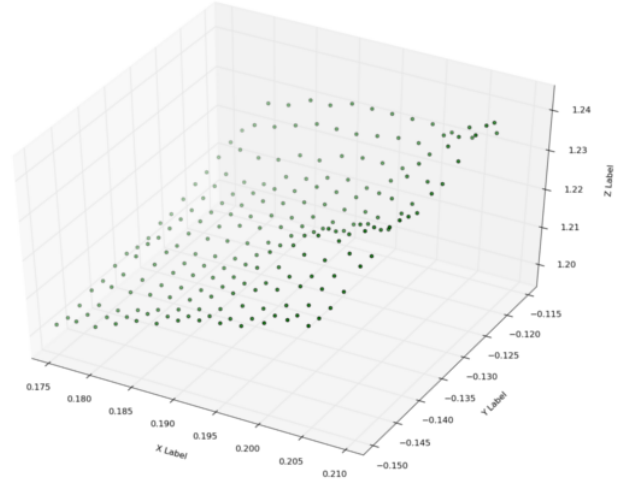

Fig. 4: The depth points of the Apriltag plane. The points are noisy but good for an approximate estimation.

the optimal rotation. However, the accuracy of this method largely depends on the depth accuracy of the chosen corner point.

An alternative is to use all 4 detected corners as 4 pairs of point correspondences for the optimization. We projected the detected corners onto $D[\hat{\boldsymbol{n}}, d]$ to get the coordinates $\boldsymbol{p} = [p_1, p_2, p_3, p_4]$ in the robot sensory frame. The corner coordinates $\boldsymbol{q} = [q_1, q_2, q_3, q_4]$ in the tag frame can be easily calculated since the tag is a square plane. We define the center of the tag as the origin, the corner coordinates are simply the location of the corners on a Cartesian plane. Given two sets of 3D point correspondences, this can be computed as a rigid body transformation estimation [Reference to SVD 3D rigid body]. Solving for the optimal transformation $[R, \boldsymbol{t}]$ requires minimizing a least squares error objective function given by:

$$[R, \boldsymbol{t}] = \operatorname*{argmin}_{R \in SO(3), \boldsymbol{t} \in \mathbb{R}^3} \sum_{i=1}^{n} w_i \|R\boldsymbol{q_i} + \boldsymbol{t} - \boldsymbol{p_i}\|^2 \qquad (3)$$

There are numerous approaches to solve Eq. 3. Since we have very few correspondences and they are assumed to be correct, it can be computed quickly using SVD:

$$\bar{p} = \frac{1}{N} \sum_{i=1}^{N} p_i \qquad p_{ci} = p_i - \bar{p} \qquad (4)$$

$$\bar{q} = \frac{1}{N} \sum_{i=1}^{N} q_i \qquad q_{ci} = q_i - \bar{q} \qquad (5)$$

$$p_c^\top q_c = U\Sigma V^\top \qquad (6)$$

$$R = VU^\top \qquad (7)$$

$$\boldsymbol{t} = \bar{q} - R\bar{p} \qquad (8)$$

R and t are the corresponding rotation and translation components of the the transformation. The above approach minimizes the least square error of the transformation and it is robust to small errors in the correspondences. The resulting pose obtained from the range data, although not accurate, is robust to noise and provide a good approximation for the true pose.
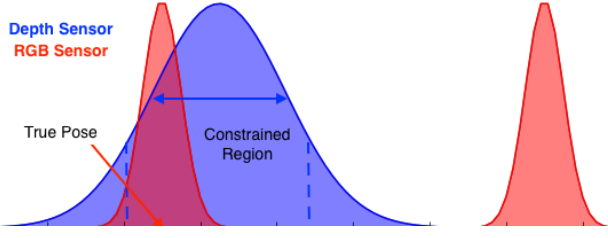
Fig. 5: An abstract visualization of the optimization constraints. The blue curve is the initial pose estimation obtained from the depth plane. The red curves are the ambiguous poses from the RGB image. We constrained the region of optimization based on how well we fit the depth plane.

C. Pose Refinement

Given the initial pose estimate of the tag and the RGB image, we can refine the pose that minimizes the reprojection error. Given camera model K, initial rotation and translation estimates R_{init} and t_{init}

$$[R^*, t^*] = \underset{R^*, t^*}{\operatorname{argmin}} \sum_i^n \|(K[R^*|t^*])p_i - y_i\|^2 \quad (9)$$

$$R^* = R + \Delta R \quad (10)$$

$$t^* = t + R\Delta t \quad (11)$$

subject to:

$$\Delta R < \Gamma_R \quad (12)$$

$$\Delta t < \Gamma_t \quad (13)$$

The challenge here is to determine the region Γ_R and Γ_t which the initial pose estimate can be adjusted. If we unbound ΔR and Δt intheon Apriltag detection algorithms on Apriltag detection algorithm the optimization, the solution might converge to a pose optimal for the reprojection error but far away from the true pose due to perceptual ambiguity. On the other hand, if we constrain the optimization too much, the final pose might not be far away from the true pose because of the inaccurate initial estimation. We recognize that the bound of on this optimization is related to the variance of the initial pose estimation. In one extreme, if there is no uncertainty in the depth camera and the range data are perfect, we don't need to further refine the pose of the tag. Similarly, if we don't have any depth information (uncertainty of the initial estimate is infinity), then the best we can do is find the pose solely based on the reprojection error which is the same as solving the unbounded optimization problem. Thererfore, this becomes a constrained optimization problem where the bound on the independent variables of ΔR and Δt is proportional to the covariance of our estimated depth plane parameters. In our implementation, we used the trust-region algorithm to bound the optimization. The scaling threshold parameter is emperically tested to yield the best results for our robot.

The key insight to our method is that it harness the different strength of RGB and depth information during the pose optimization process. By considering all the points on the tag, the depth data is more robust to noises in the scene. However, range data is inherently inconsistent and the pose is thus imprecise. In contrast, the advantage of RGB image

is that the corners can be detected at a sub-pixel precision. It is useful for refinement optimization.

V. EXPERIMENTAL RESULTS

The key problem we are trying to resolve is the localization accuracy of Apriltags in noisy situations. There are two major components we want to demonstrate in this paper: first, we want to characterize the effect of perceptual ambiguity and noise on the Apriltag detection algorithms. Second, we want to test the resilience of our algorithm and show that it can obtain reasonable pose estimations under high level of noise. Finally, we briefly tested the runtime of the algorithm to show that it remains capable of real time detection.

In our experiments, we measured the rotational and translational accuracy of the detections algorithms with respect to three different independent variables: viewing angles, distances, and lighting conditions. We placed a standard camera calibration chessboard and an Apriltag of known size on a solid planar board. The Apriltag has a fixed distance from the chessboard. This is used to compute the ground-truth pose for the tag. By using a large chessboard, we can detect the corners to a sub-pixel accuracy and compute accurate ground-truth poses unsusceptible to lighting and sensory noises. Figure 9 demonstrates the experimental set up.

A. Viewing Angle

The low localization accuracy caused by the perceptual ambiguity of the Apriltags is a non-linear function on the viewing angle of the tag. To characterize the effect, we placed the testing board on a table straight in front of the robot in a well lit room. Since the sensor is taller than the plane of the table, the robot has to slightly gazing down at it. We rotated the testing board at a increment of 5 degrees from 0 degrees to 70 degrees. This is about the range in which the tag can be detected reliably given the camera resolution and distance. At each angle, we captured the RGB image, depth image, and detection outputs from the Apriltag algorithm.

For each captured data collection, we introduced 3 levels of Gaussian noise of $\sigma = 0.2$, $\sigma = 0.5$, $\sigma = 1$ to the RGB image and computed the resulting tag pose. This is repeated for 1000 trails at each noise level and the errors are computed for each trial. Figure 6 shows some of the results.

As the result shown in figure 7 indicates, the viewing angle has large effect on the rotation error. As we expected, the empirical results show a very clear bimodal distribution for the Apriltags at different viewing angles. The depth-sensor fused algorithm vastly outperforms the previous algorithm as it is not affected by the perceptual ambiguities. The small amount of the noise introduced to the data only cause a small rotational change around the true pose of the tag. In Figure[8], we threshold all the poses based on their rotational errors and plotted the percentage of unacceptable poses at each viewing point. One interesting observation from the data is that, at most viewing angles, the magnitude of noise above a certain threshold has little effect on the localization accuracy. At most viewing angles, relatively small noises causes a significant accuracy decrease.
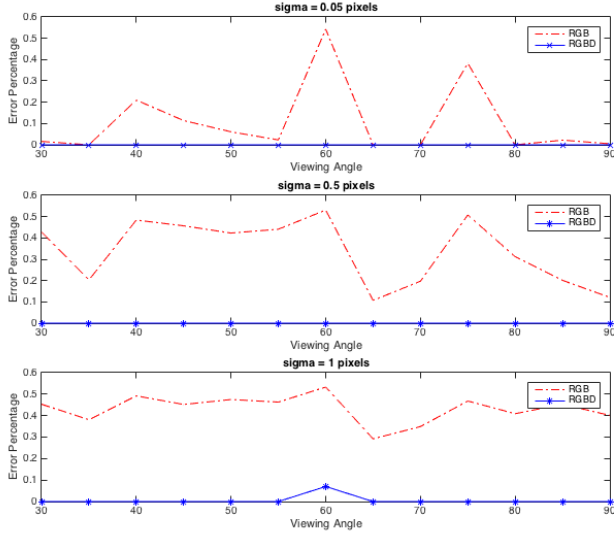
Fig. 6: Viewing Angle vs Error Percentage under different simulated noise level. The new RGBD based algorithm can resist noise in the RGB image and it vastly outperforms the original algorithm.
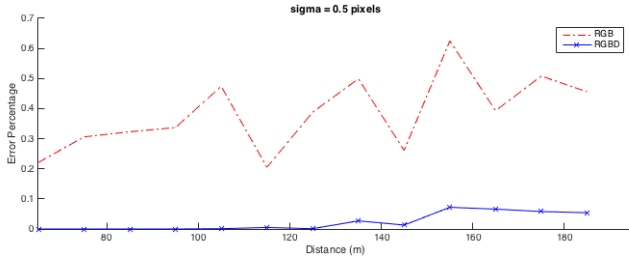

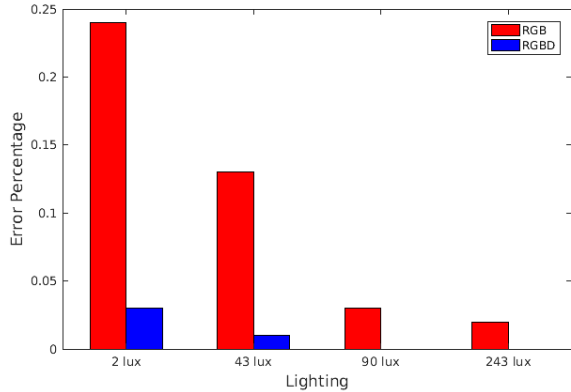Fig. 7: Distance vs Error Percentage. Data are captured at a 10 cm increment from 65 cm to 185 cm.

Fig. 8: Illumination vs Error Percentage. Data are captured at 65 cm away from the camera at a 40 degree angle.

B. Distance

In additional to the viewing angle, we captured the images at different distances away from the camera at a fixed angle. Figure 7 shows the experiment results.

The relationship between the distance and localization accuracy is much more apparent. As the tag moves further away from the sensor, the number of pixels on the tag decreases. The perspective ambiguity effect becomes more apparent when there is only a small patch of pixels on the tag. However during the experiment, it is difficult to keep the viewing angle precisely consistent at each trail. Therefore, the pose error percentage using RGB is not increasing smoothly in Figure 7.

We see a clear increase in error percentage in the proposed method when the tag is far away from the camera. This is contributed both by a smaller tag patch size in the depth image and an increasing in noise with the Kinect sensor at a further distance. In these cases, the variance of the depth plane estimation became very wide and the algorithm is unable to converge to the correct pose. The Nevertheless, our method has a significant gain in accuracy at every distance.

C. Lighting

From our past observations, poor lighting condition is the most significant contributing factor to sensory noise and it results in low localization accuracy. The Kinect V2 sensor used in our experiments dynamically adjust the exposure time under low lighting conditions. The images produced contain very noticeable noise as shown in Figure **??**.

Therefore, we also tested the algorithm under harsh lighting conditions in a real world setting. The data were captured under 4 different lighting conditions: 20 lux (dark), 43 (lux) dim, and (90 lux) normal, 243 lux (bright). As results shown in Figure 8, the localization accuracy significantly improves with better illumination.

The Kinect sensor automatically adjusts the exposure settings to compensate for the low lighting. The pictures captured in the dark rooms still appears bright but much more grainy and apparent Gaussian noise in the image. Depth sensor and RGB sensor works optimally under different lighting conditions. In the dark setting, the depth sensor performs well.

VI. DISCUSSION

A. Perceptual Uncertainty

An important problem is to formally define the perceptual uncertainty produced by any detection algorithm similar to those in SLAM. For example, if the detector knows the pose estimated have large margins of error, it is useful to have some notion of uncertainty around the estimated pose. These are especially helpful inputs to any motion planing algorithms that takes uncertainty into consideration. In our implementation, we have a loose definition of detection uncertainty. We implicitly treated the pose estimation from depth sensor and RGB sensor as two independent observations. Uncertainty of the pose can be described by the variance and differences
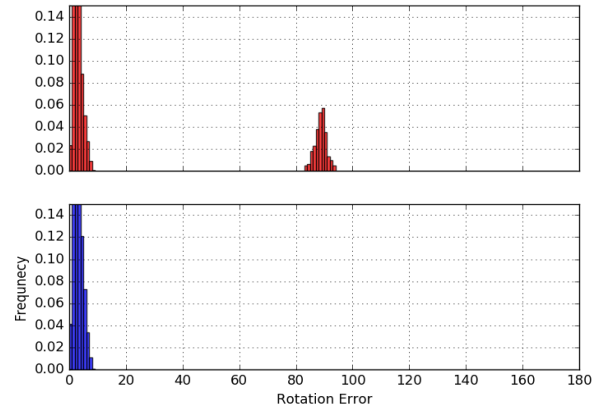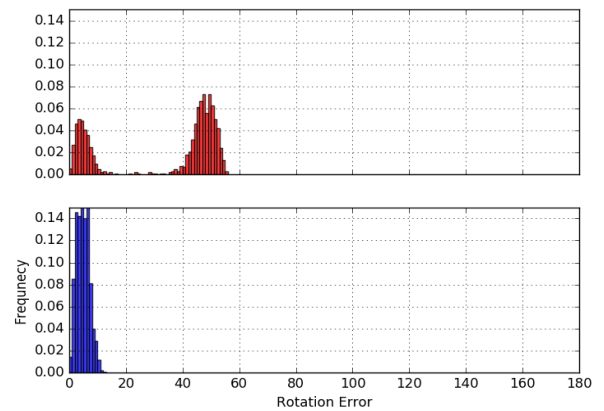
(a) RGB Image at 75°
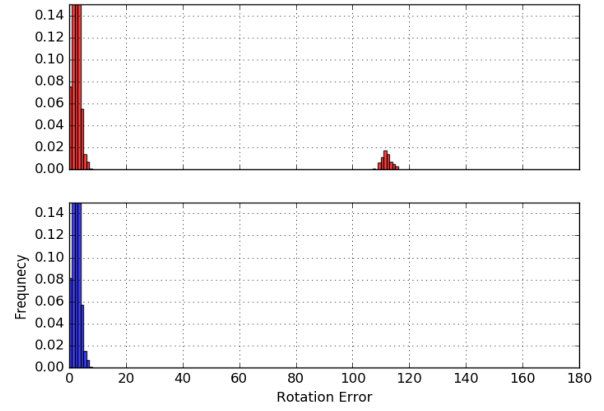
(b) Distrubtion
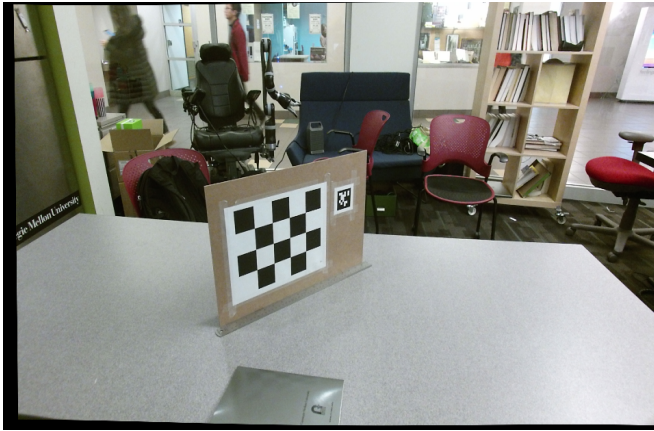
(c) RGB Image at 40°

(d) Close

(e) RGB Image at 5°

(f) Close

Fig. 9: The fiducial tag plane captured by the depth sensor

between two observations. This can be achieved using a similar technique to the updating step in Kalman filters.

B. Computation Time

We briefly tested the computation time of the new algorithm. With our current implmentation in Python, the algorithm can process a $pixel by pixel$ image in xxx seconds. All tag detectors and the fusing process were running in a single-threaded mode of an Intel core. Since our sensory updates at roughly $35Hz$, the entire pipeline can process the tags in real time. There is no signifciant time increase on a higher resolution image because our fusing algorithm does not need to process the entire image. Therefore, the only time increase comes from the initial Apriltag detection process which has been shown to work under 30 ms for large images.

The most time consuming step is running the trust region optimization for refining the pose. This process can be sped up significantly by simply implementing the pipeline in C++.

VII. CONCLUSION

In this paper, we did a in depth analysis of the localization problem with Apriltags. We proposed a novel algorithm of using RGBD sensors to accurately compute the pose of Apriltags robust to noise. It is particularly suitable for robotic applications which requires precise poses such as manipulation, SLAM, and others. Furthermore, this technique can be easily generalized to other types of planar fiducial tags. Our implementation is fully open sourced and available at:

http://somegithublink.com